ACCSCIENCE PUBLISHING

International Journal of Bioprinting

RESEARCH ARTICLE

Effect of seed distribution characteristics on mechanical properties, degradation behavior, and osteogenic differentiation of additively manufactured Voronoi-based biomimetic scaffolds

Supplementary file

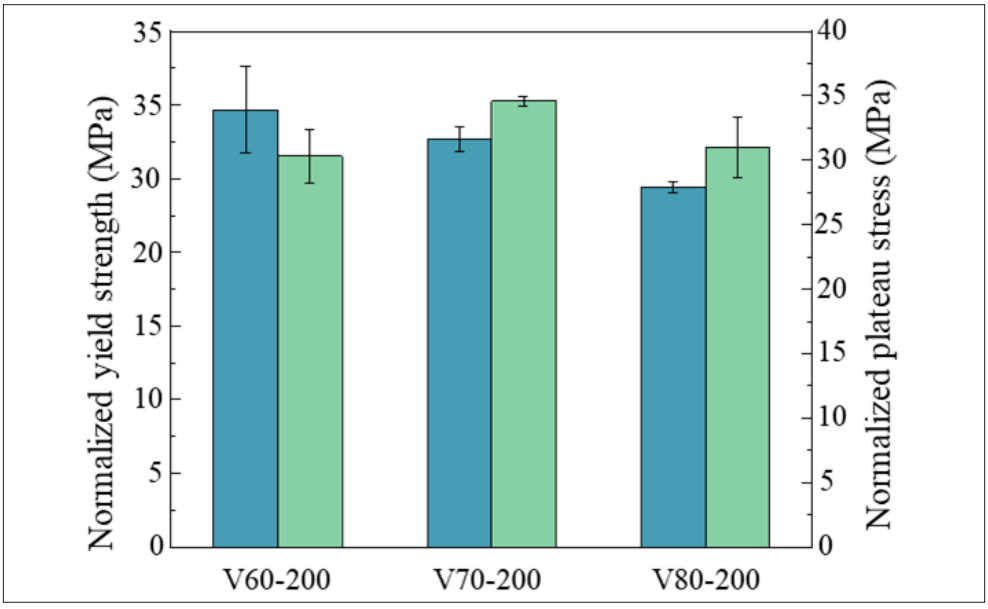

Figure S1. Normalized yield strength and plateau stress of the Voronoi scaffolds with different porosities

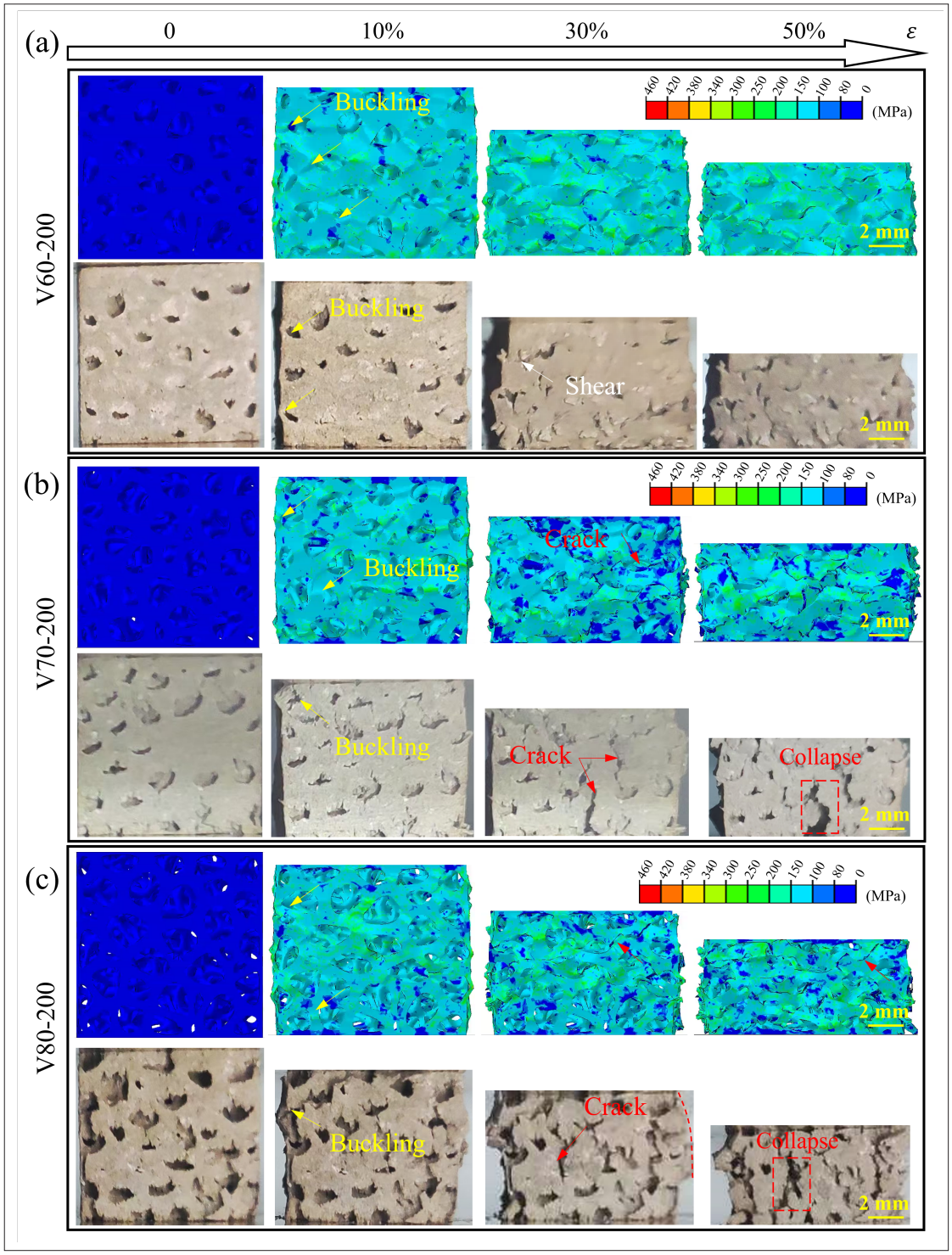

Figure S2. Simulation and experimental compressive deformation behavior of Voronoi scaffolds with different porosities under 10%, 30% and 50% strain. (a) V60-200; (b) V70-200; (c) V80-200.

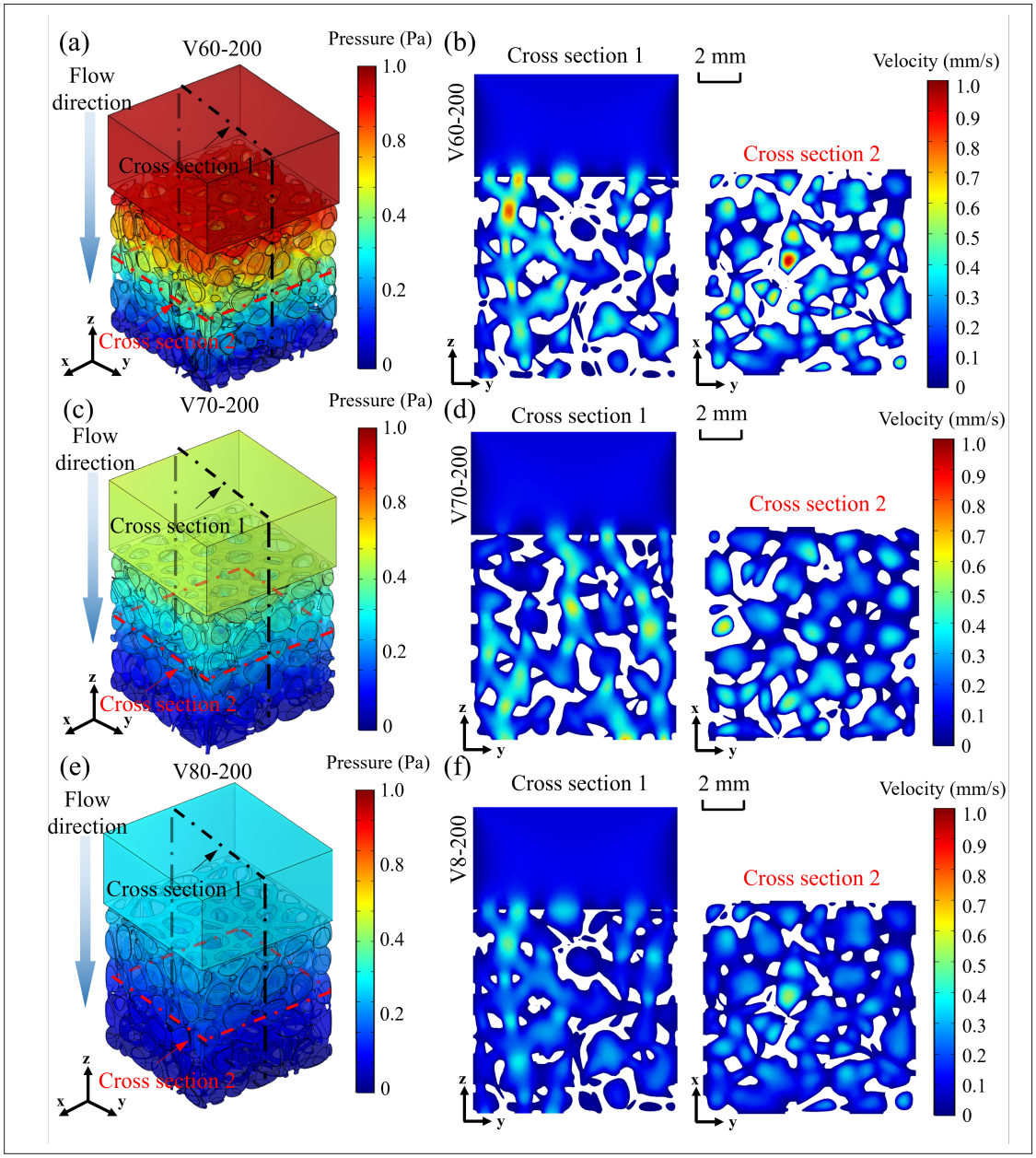

Figure S3. Fluid flow analysis of Voronoi scaffold with different porosities. (a, c, e) Pressure distribution; (b, d, f) Flow velocity distribution.

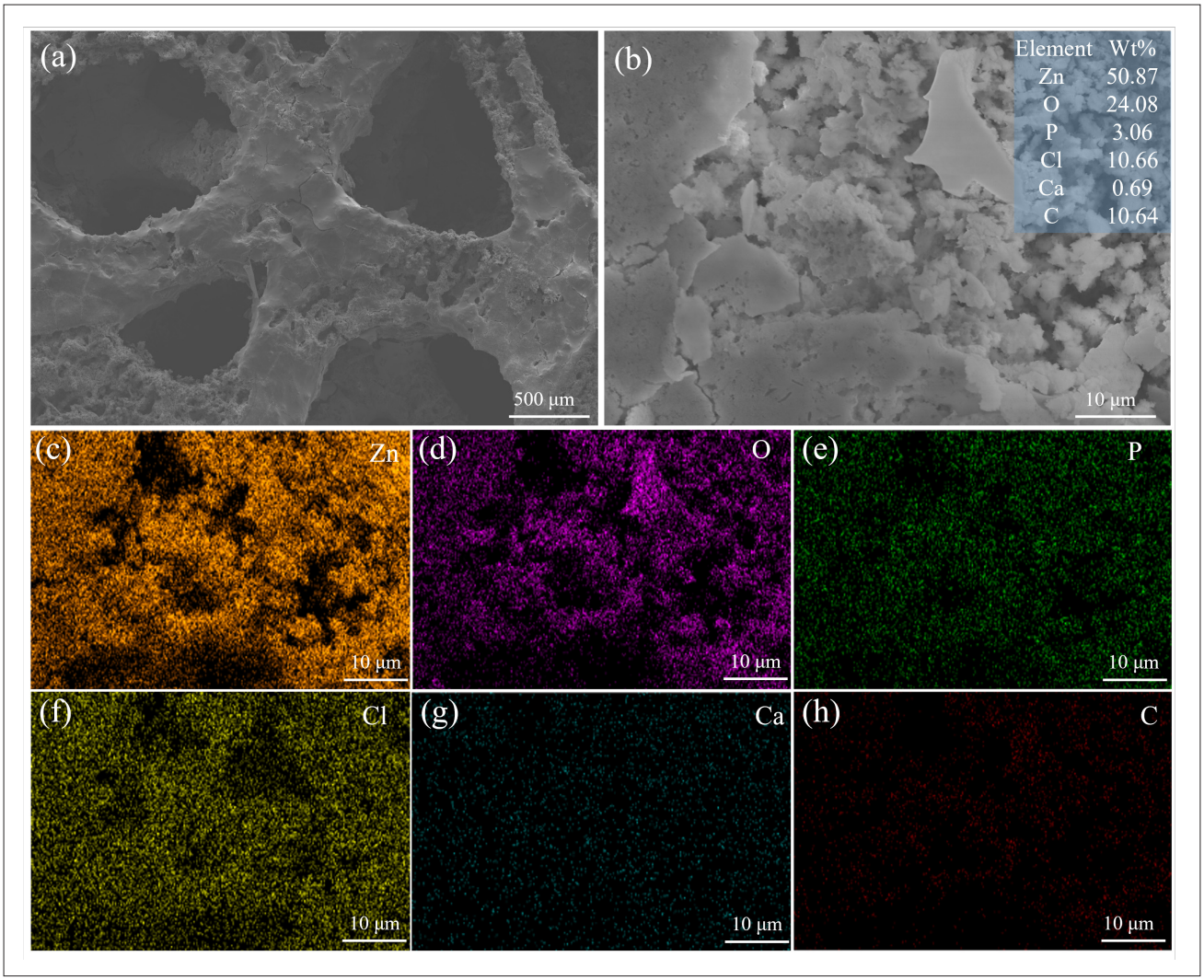

Figure S4. Analysis of degradation products of V80-200 sample on day 14. (a, b) SEM characterization; (c–h) EDS component analysis. Abbreviations: EDS: Energy-dispersive X-ray spectroscopy; SEM: Scanning electron microscopy.

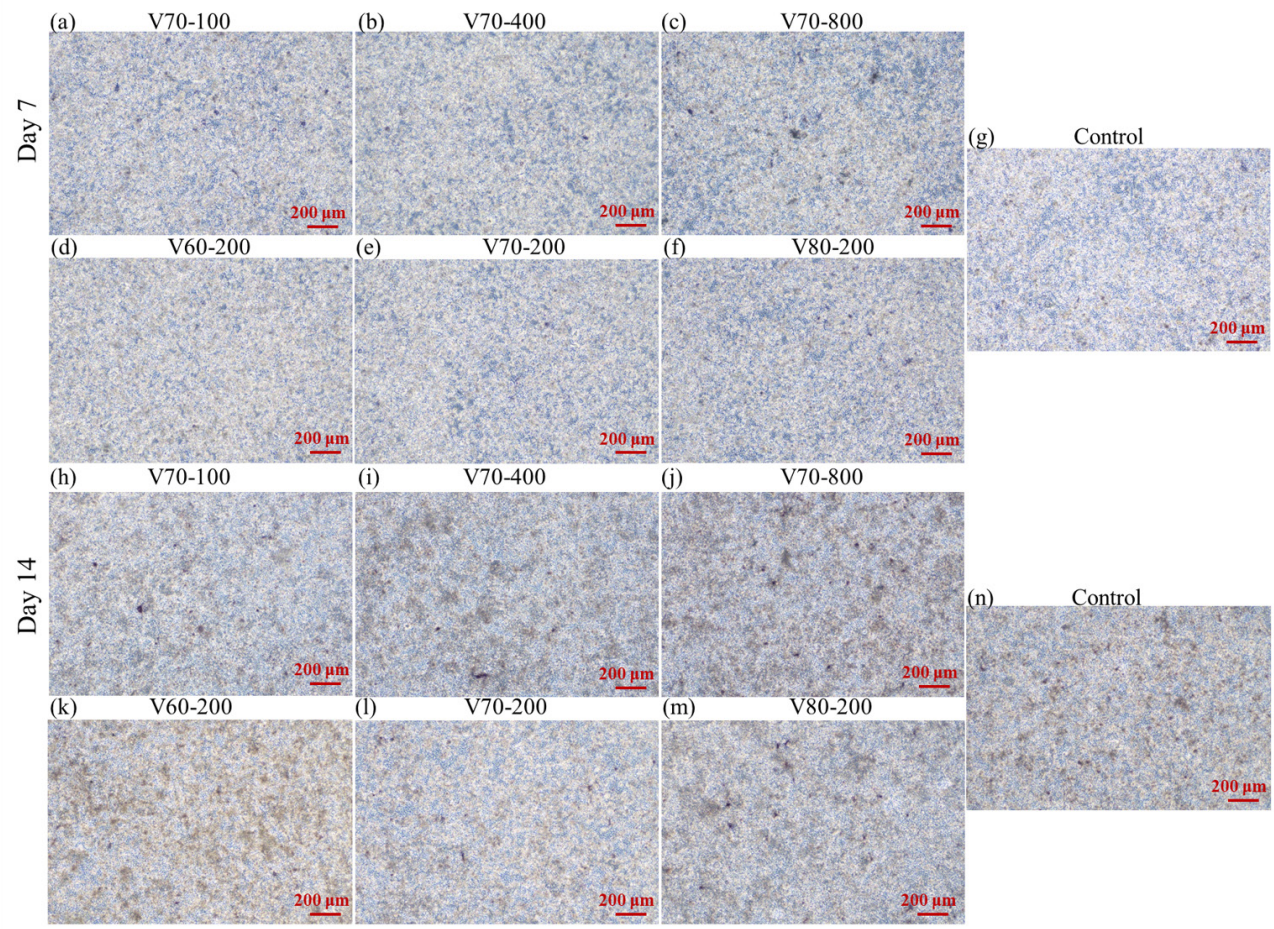

Figure S5. Alkaline phosphatase staining results for assessing osteogenic differentiation of zinc-based Voronoi scaffolds with different porosities and seed counts after days 7 and 14. (a–g) On day 7; (h–n) On day 14.

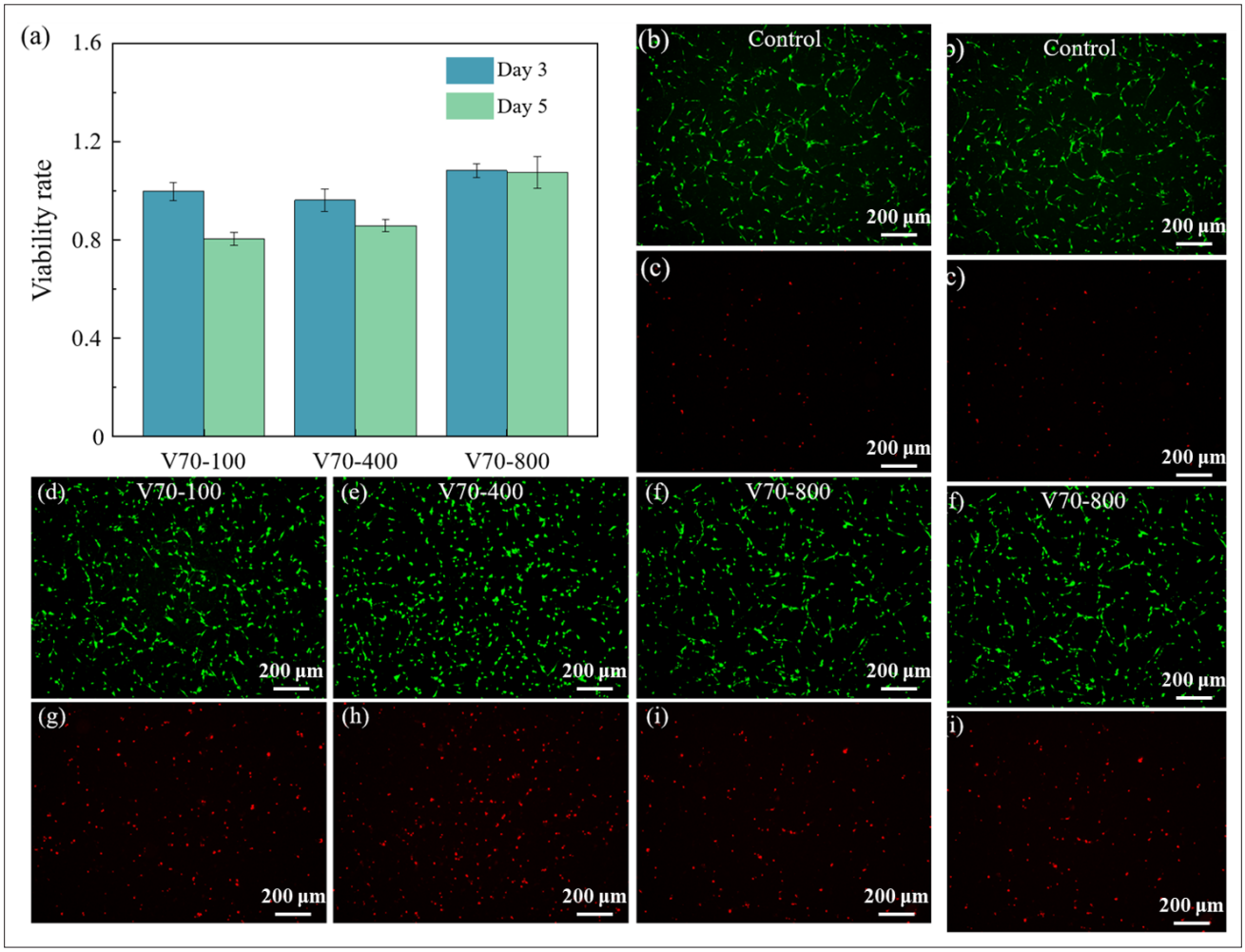

Figure S6. Effect of zinc-based Voronoi scaffolds with different seed counts on cell viability. (a) Viability rate; (b–i) Live-dead cell staining on day 5.

Table S1. Sequences of primers used in gene expression experiment

Gene	Forward primer (5' to 3')	Reverse primer (5' to 3')
COL1	CTGGCGGTTCAGGTCCAAT	CTGGCGGTTCAGGTCCAAT
ALP	CCAACTCTTTTGTGCCAGAGA	GGCTACATTGGTGTTGAGCTTTT
OCN	CTGACCTCACAGATCCCAAGC	TGGTCTGATAGCTCGTCACAAG

Table S2. Comparative analysis on the mechanical properties and permeabilities of the scaffold in this study with other scaffolds reported in previous studies

Scaffold type	Young's modulus (GPa)	Yield strength (MPa)	Permeabilities ($\times 10^{-9}$ m^2)
Trabecular bone	0.462–1.181	1–16	0.75–7.43
Ti6Al4V Gyroid[1-3]	0.2–1.4	5–13	1.2–1.4
Zn Diamond[4,5]	0.75–1	11–11.5	0.7–1.1
Ti6Al4V PM[6]	0.59–2.9	20.59–112.63	9.87–49.19
316L Gyroid[7]	2.04–2.71	55.0–89.4	27.4–40.3

References

1. Wang C, Hu Y, Zhong C, et al. Microstructural evolution and mechanical properties of pure zinc fabricated by selective laser melting. *J Mater Sci Eng* 2022;846:143276. doi: 10.1016/j.msea.2022.143276
2. Liu F, Mao Z, Zhang P, *et al*. Functionally graded porous scaffolds in multiple patterns: new design method, physical and mechanical properties. *J Mater Des*. 2018;160:849-860. doi: 10.1016/j.matdes.2018.09.053
3. Ma S, Tang Q, Han X, *et al*. Manufacturability, mechanical properties, mass- transport properties and biocompatibility of triply periodic minimal surface (TPMS) porous scaffolds fabricated by selective laser melting. *J Mater Des*.2020;195:109034. doi: 10.1016/j.matdes.2020.109034
4. Li Y, Pavanram P, Zhou J, *et al*. Additively manufactured biodegradable porous zinc. *J Acta Biomater*. 2020;101:609-623. doi: 10.1016/j.actbio.2019.10.034
5. Santos J, Pires T, Gouveia B, *et al*. On the permeability of TPMS scaffolds. *J Mech Behav Biomed Mater.* 2020;110:103932. doi: 10.1016/j.jmbbm.2020.103932
6. Zhang L, Song B, Yang L, *et al*. Tailored mechanical response and mass transport characteristic of selective laser melted porous metallic biomaterials for bone scaffolds. *J Acta Biomater.* 2020;112:298-315. doi: 10.1016/j.actbio.2020.05.038
7. Ma S, Tang Q, Feng Q, *et al*. Mechanical behaviours and mass transport properties of bone-mimicking scaffolds consisted of gyroid structures manufactured using selective laser melting. *J Mech Behav Biomed Mater*. 2019;93:158-169. doi: 10.1016/j.jmbbm.2019.01.023